

COVID-19 detection using deep convolutional neural networks and binary-differential-algorithm-based feature selection on X-ray images

Mohammad Saber Iraj^{a,c}, Mohammad-Reza Feizi-Derakhshi^{b,*}, Jafar Tanha^c

^a *Department of Computer Engineering and Information Technology, Payame Noor University, Tehran, Iran*

^b *Computerized Intelligence Systems Laboratory, Department of Computer Engineering, University of Tabriz, Tabriz, Iran*

^c *Department of Computer Engineering, University of Tabriz, Tabriz, Iran*

Corresponding author: Mohammad-Reza Feizi-Derakhshi (mfeizi@tabrizu.ac.ir)

Abstract

The new Coronavirus is spreading rapidly, and it has taken the lives of many people so far. The virus has destructive effects on the human lung, and early detection is very important. Deep Convolution neural networks are such powerful tools in classifying images. Therefore, in this paper, a hybrid approach based on a deep network is presented. Feature vectors were extracted by applying a deep convolution neural network on the images, and useful features were selected by the binary differential meta-heuristic algorithm. These optimized features were given to the SVM classifier. A database consisting of three categories of images such as COVID-19, pneumonia, and healthy included in 1092 X-ray samples was considered. The proposed method achieved an accuracy of 99.43%, a sensitivity of 99.16%, and a specificity of 99.57%. Our results demonstrate that the suggested approach is better than recent studies on COVID-19 detection with X-ray images.

Keywords— *Deep convolution, COVID-19, Meta-heuristic, Binary differential, Neural networks, X-ray image*

1. INTRODUCTION

The rapid spread of COVID-19 has killed many people around the world. The disease is associated with symptoms such as muscle aches, coughs, fever, and can be detected through clinical trials and radiographic imaging. Medical imaging is very essential in diagnosing diseases. The X-rays and computed tomography (CT) scans of the disease can be used in the deep network to help diagnose the disease more quickly.

The process of classifying and diagnosing the disease from a photo using a neural network consists of 4 main steps: feature extraction, optimal feature selection, network training, and model performance test. Feature extraction is of two types. In the first case: The feature extraction process is done using image processing techniques, algorithms, and filters. The extracted features from images include the shape of tissues and the texture used for patient classification. In the second type, the original images and their actual output class were entered into the convolution network as input data, and after the network training process and weight adjustment, the features were automatically extracted in the last flatten layer.

Some features extracted from the deep network may have a detrimental effect on classification accuracy [1]. Therefore, the optimal feature selection methods are essential. There are three types of feature selection methods. The filter method uses the intrinsic properties of features and statistical indicators such as fisher score, information gain, chi-square, correlation coefficient. The wrapper method uses a learning algorithm and looks for a subset of features in the feature space that optimize classification accuracy. Therefore, wrapper approaches use meta-heuristic methods for feature subset selection and cross-validation. The hybrid method applies a combination of filter and wrapper methods [2]. Among the feature selection methods, meta-heuristic methods have shown better performance in applications with lots of features [3].

Analyzing extracted features from images and selecting optimal features improves classification performance [4]. In the field of medical imaging, it has been reported many feature selection (FS) studies such as Robustness-Driven FS (RDFS) for lung CT image [5] • Shearlet transform FS from brain MRI image [6]• principal component analysis for lung X-Ray Images [7], genetic algorithm (GA) for lung nodules [8]• bat algorithm (BA) compared with particle swarm optimization (PSO) in lung X-ray images [9], flower pollination algorithm (FPA) from lung images [10].

In the study above, using different available methods for classifying patients from lung images by machine vision combined with meta-heuristic algorithms is propounded. On the other hand, existing diagnostic methods for COVID-19 disease with X-ray images use high memory, long time, and many features. Therefore, an intelligent system seems to be necessary, which helps physicians and treatment staff to classify COVID-19 patients with high accuracy and high speed to reduce mortality from the disease. The motivation of the research is to plan an efficient procedure with artificial intelligence methods to aid doctors and patients in COVID-19 prediction with high accuracy. The novelty of the research is the design of deep learning structure based on feature selection, by using the binary differential evolution algorithm in COVID-19 diagnosis. The contributions of the study are as:

1- Designing an intelligent system using the deep convolutional neural network without a pre-trained network based on lung X-ray images and extracting features from it with the minimum optimal memory required to create and train the network.

2- Selecting the optimal features of the differential meta-heuristic method that led to the improvement of the performance indexes

3- Increasing the classification accuracy for multi-class problems, including three categories of patients with COVID-19, pneumonia, and healthy.

The structure of our study is as follows: related works are reviewed in section 2. In section 3, the proposed methodology and model using deep convolution and binary differential algorithm for COVID-19 detections is presented. Experimental results are shown in section 4. Discussion and comparison with other previous works are described in section 5. Finally, the study ends with a conclusion.

2. RELATED WORKS

Hemdan, Shouman, & Karar have suggested the positive or negative status of COVID with deep learning models [11]. They had reported that the VGG19 model has better results with 90% accuracy on 25 COVID, 25 non-COVID images. Toğaçar, Ergen, & Cömert have used 295 COVID, 98 pneumonia, 65 normal images into MobileNet and SqueezeNet [12]. They have extracted features from the trained Net models, and then the features were selected by the SMO algorithm. The overall accuracy was 99.27% using the SVM classifier. Zhang, Xie, Li, Shen, & Xia investigated a ResNet model with 18 layers for 100 COVID, 1431 pneumonia images. The value of accuracy reached 95.18% [13]. Apostolopoulos & Mpesiana offered pre-trained VGG19 based on 224 COVID, 700 pneumonia, 504 normal images [14]. The accuracy of their results was 98.75%. In [15], the authors considered the DarkNet with 17 convolutional layers using 127 COVID, 500 pneumonia, 500 normal images, and the accuracy was 98.08%. In [16], the performance of CNN was improved using preprocessing image algorithms, and the model resulted in 94.5% accuracy.

In [1], the authors designed a COVID-19 classification method which mixed a CNN named Inception pre-trained Imagnet as feature extractor and Marine Predators Algorithm as feature selector, KNN as classifier based on two datasets. Dataset1 included 200 COVID-19 positive images and 1675 negative also, dataset2 contained 219 COVID-19 positive images and 1341 negative images. Accuracy was stated 98.7%, 99.6% for dataset1, dataset2. Canayaz checked a COVID-19 diagnosis model using VGG19, ResNet, AlexNet, and GoogleNet mixed by two meta-heuristic algorithms named binary particle swarm optimization and binary gray wolf optimization. The best overall classification accuracy was 99.38% after feature selection by binary gray wolf optimization based on 1092 X-ray images of COVID-19, pneumonia, and healthy records [17].

One of the limitations of the previous works is the use of pre-trained deep networks that require plenty of memory. In addition, a large number of input features and long detection time are other shortcomings. To improve the detection of COVID-19 by overcoming the above limitations, we proposed the deep learning approach based on feature selection using the binary differential evolution algorithm method.

3. METHODOLOGY AND MODEL

The proposed model is shown in Figure 1. First, the lung images enter into the convolutional neural network. After training the network, features are extracted from the images that are not optimal. Optimal features are extracted using the heuristic method. The classification of the three classes named COVID-19, pneumonia, and healthy is done with higher accuracy.

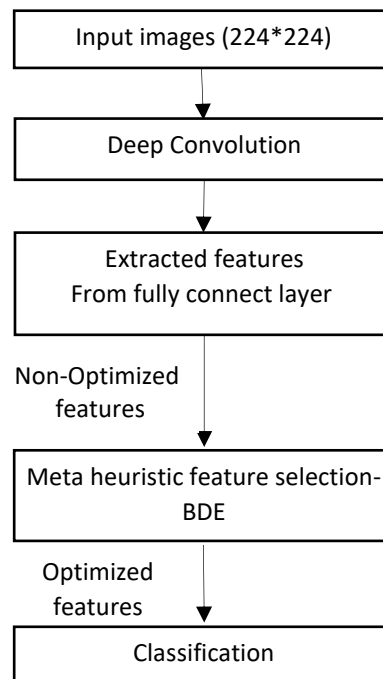


Figure 1. The proposed model for COVID-19

2.1. Deep convolution

The convolution neural network is a features extractor and a suitable classification method in machine learning. In the convolutional network, the input of the network is the original data, such as images. The network automatically extracts the features, through the convolution function, after learning, instead of extracting the feature manually, the matrixes as the filters, slide on the main input image, and the convolution operation is

performed through equation 1. Finally, after training and mapping the input images to the output labels, the features are extracted after several convolution layers [18].

$$(IMG * C)_{ij} = \sum_{p=0}^{c_1-1} \sum_{q=0}^{c_2-1} \sum_{c=1}^{tc} C_{p,q,c} \cdot IMG_{i+p,j+q,c} + bs \quad (1)$$

where IMG is input image with height=H, width=W dimensions, tc is the number of image channels, C is filter matrix with $c_1 \times c_2$ dimensions, bs is a bias value for each filter C, $i=0 \dots H$, $j=0 \dots W$

After applying the convolution, the unwanted values are removed with the ReLu layer, and then the input is reduced by the pooling layer. The effective input vector enters the fully connected layer, which has the same function as the MLP. In the final part of the deep convolution layers, Softmax [19], classification layers, perform

the classification operation using ADAM (adaptive moment optimizer) [20], lost function is in bellow (equation 2).

$$L(w, b) = -\frac{1}{M} \sum_{m=1}^M [y_m \log \hat{y}_m + (1 - y_m) \log(1 - \hat{y}_m)] + \Gamma \times \sum_{r=1}^M \|w^r\|_2 \quad (2)$$

where M is the number of sample images, y_m is an actual class for the m-th sample, \hat{y}_m is the predicted output class for m-th input data, Γ is the regularization coefficient.

ADAM is an optimization algorithm that calculates the exponential moving average of gradient and square of the gradient to update neural network weights and, effectively solve deep network issues. The deep neural network consists of many different layers in which there are many learning parameters, namely weights and biases. Applying the optimal feature selection algorithm and then applying it to the ADAM optimizer increases the speed and accuracy of the optimization [21].

2.2. Binary Differential Evolution

Differential evolution (DE) [22] is an evolutionary heuristic method designed for minimizing the continuous problem. Binary differential evolution (BDE) [23] is expanded for feature selection issues. It has three prominent builders named mutation, crossover, and selection. First, the initial population is produced by dimensions D, which D is the number of features we want to optimize. For the mutation operation, three random vectors p_{u1}, p_{u2}, p_{u3} are selected for vector p_k such that $u1 \neq u2 \neq u3 \neq k$, k is a vector arrangement in population.

If the d-th dimension of a vector p_{u1} and vector p_{u2} be equal, the d-th feature of the difference vector (equation 3) will be zero; otherwise, it takes the same value as a vector p_{u1} .

$$difference\ vector_k^d = \begin{cases} 0 & p_{u1}^d = p_{u2}^d \\ p_{u1} & other \end{cases} \quad (3)$$

Afterward, the mutation and crossover are executed as shown in equations 4 and 5.

$$mute\ vector_k^d = \begin{cases} 1, & \text{if } difference\ vector_k^d = 1 \\ p_{u3}^d, & \text{other} \end{cases} \quad (4)$$

$$W_k^d = \begin{cases} mute\ vector_k^d, & \text{if } \gamma \leq CR \ \parallel \ d = d_{random} \\ p_k^d, & \text{other} \end{cases} \quad (5)$$

where W is the try vector, $CR \in (0, 1)$ is crossover amount, and $\gamma \in (0, 1)$ is a random number. In the selection procedure, if the fitness value of the try vector W_k is greater than the current vector p_k , we will replace it. Otherwise, the current vector p_k is stored for the next generation.

4. EXPERIMENTAL RESULTS

4.1. Description of data

Canayaz created a COVID-19 X-ray data set including three classes of patients with COVID-19, pneumonia, and healthy [17]. In this database, there are 364 images for each of the three categories obtained as a balanced dataset by combining data [24-26]. The total number of images are equal to the number of classes multiplied by the number of class instances, hence $(3 \times 394)1092$, and its dimensions are 224×224 . In this study, the same data is used to predict COVID-19 disease with the convolutional neural network and to select optimal features by the meta-heuristic algorithm named binary differential. Figure 2 shows one sample of three output classes as COVID-19, pneumonia, and healthy.



Figure 2. The Chest X-ray images of different conditions (a) COVID-19 (b) Pneumonia (c) Healthy

4.2. Performance evaluation

The suggested model was performed in Matlab version 9.1.0.441655 (R2018b) on a notebook PC with, 1.8 GHz CPU, and 4 Gigabyte RAM. The proposed method takes an average of 29 seconds per patient after training in the application phase, which can be reduced by improving the used hardware technology [18, 19]. The accuracy, sensitivity, specificity, geometric mean, and area under curve (AUC-ROC) [29, 30] as performance evaluation metrics (equations 6-9) were considered to measure the COVID 19 prediction model. The correctness of classification is named accuracy. The amount of the negative cases that are correctly distinguished is “specificity”; the amount of the positive cases that are correctly distinguished is “sensitivity”. The second root of

the product of sensitivity, specificity, is called the geometric mean. Higher values of the area under the curve (AUC) in the receiver operating characteristics indicate better classification performance.

$$Accuracy = \frac{TP+TN}{TP+TN+FP+FN} \quad (6)$$

where:

True positives = the number of samples that are correctly labelled as positive

False positives = the number of samples that are wrongly labelled as positive

True negatives = the number of samples that are correctly labelled as negative

False negatives = the number of samples that are wrongly labelled as negative

$$Sensitivity = TP / (TP+ FN) \quad (7)$$

$$Specificity = TN / (FP+TN) \quad (8)$$

$$Geometric\ mean = \sqrt[2]{Sensitivity * Specificity} \quad (9)$$

4.3. Model parameters

The structure of the deep convolution neural network is shown in Figure 3. Firstly, the dimensions of images in the image input layer were 224*224; and there were eight filters 3-by-3 for the convolution operator. The local features are automatically extracted after processing the first block of the network layers, i.e., image input, convolution, Batch Normalize, ReLU, max-pooling layers, fully connected layer 400, ReLU, Drop out. Finally, the second network block, including three- fully connected layers, softmax, classification, categorizes the input images into three output classes. The validation accuracy after 200 epochs was 97.25% using ADAM optimizer during training, and the mini-batch size was 64 (Figure 4). The batch normalization and dropout are put due to regularization of the neural network and barricade overfitting.

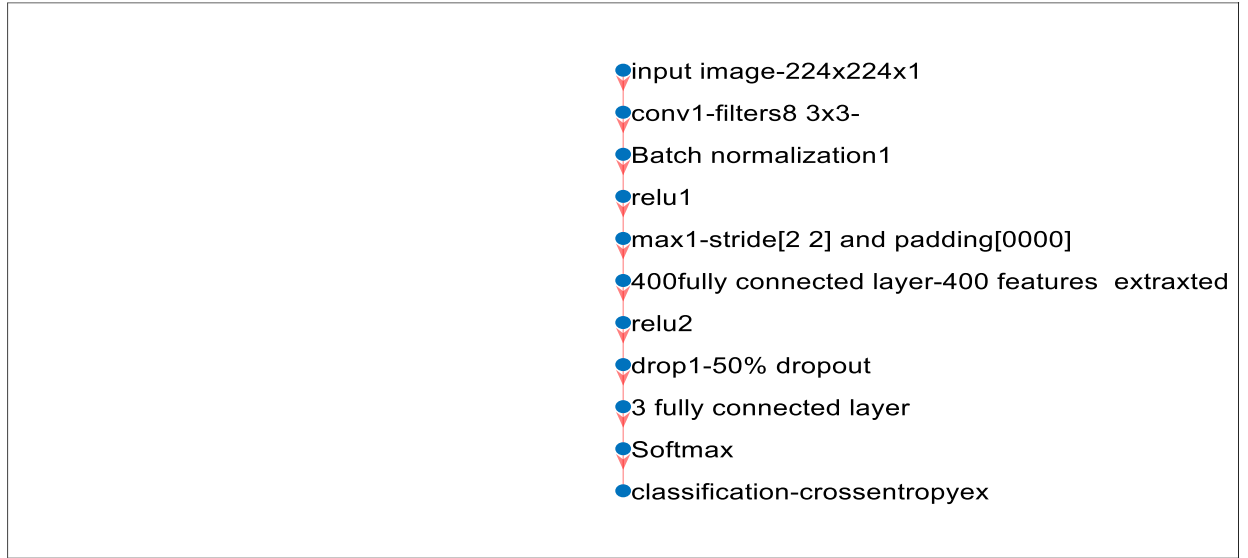


Figure. 3. Structure of proposed model layers

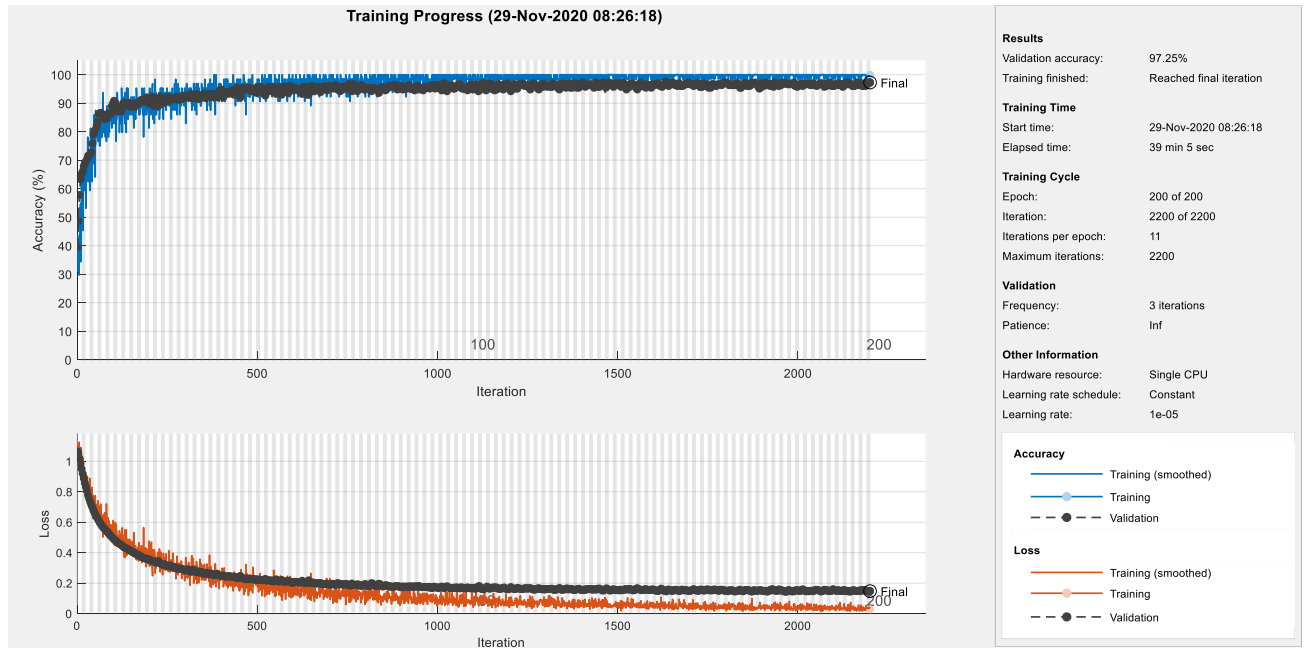


Figure. 4. Accuracy and loss measure for training, validation data using convolution neural networks

Convolution networks are methods for converting the input to feature vectors. Since some network features may cause poor performance for the model [1], after extracting 400 features in the first fully Connect layer, the meta-heuristic algorithm named binary differential was used to select the optimal features subset and remove the useless features. In the binary differential algorithm, population = 20, iteration= 100 (figure 5), and a crossover rate of 1 were the algorithm's parameters. Amount (1- (geometric mean)) of the SVM classifier [31] was considered as fitness values of the population (Figure 5). After executing the binary differential algorithm, 340 optimal features were selected.

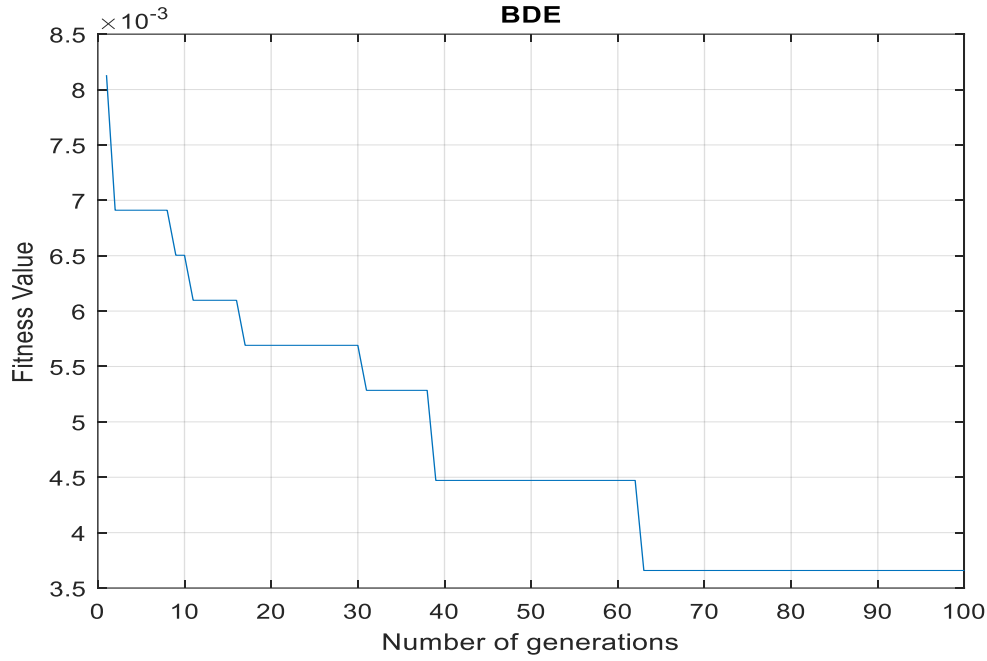


Figure. 5. Fitness curve for the Binary differential algorithm

4.4. Performance comparison

The conventional validation (CV) method using random sampling is one of the training and testing protocols to compute the model accuracy and validation of the estimation results. According to the CV method, 70% of the data was considered for training, 15% for the validation, and 15% for the test [32, 33]. The proposed method was applied to the data and 100 runs is done to prevent overfitting [34]. Both the optimal selected features by the differential algorithm and the initial extracted features from the deep convolution neural network, entered into the SVM classifier.

Table 1 demonstrated the confusion matrix using training, testing, validation, and total data for original features, and optimized features applied by the SVM classifier. The TP, TN, FP, FN, accuracy, sensitivity, specificity, geometric mean, AUC metrics for each of the three output classes, and each type of testing, training, validation, and total data were computed (Table2).

5. DISCUSSION

Applying images to a deep neural network can be used to predict disease. In other words, a deep neural network can be exerted as a feature extractor. The large size and high volume of applied images to the deep neural network produced many features that prolonged the training time and decision time of the predictive model.

The design challenges of the proposed model were: first: collecting lung images and improving them. Secondly, deep network architecture, including structure, number, and type of layers. Third, the meta-heuristic algorithm,

the initial population, and the objective function type of the meta-heuristic algorithm. The presence of inefficient features extracted from the deep network could reduce the accuracy and efficiency of the predictive model. Therefore, selecting the optimal features by the meta-heuristic method improved the memory, time, and accuracy of the model.

According to Table 3, the proposed model based on the extracted features from the X-ray image using CNN and selected optimized features by the binary differential meta-heuristic algorithm has attained an accuracy of 99.43%, a sensitivity of 99.16%, a specificity of 99.57%, a gmean of 99.37%, AUC of 0.99, and a root mean square error (RMSE) of 0.1133. In this paper, accuracy for the classification of the COVID -19 issue was calculated to be 99.43%, and the count of relevant features was 304 (Table 4), whereas in the previous study [17], based on the same data, they were reported to be 99.38%, 448 features.

Transfer learning models are trained to categorize 1,000 categories of images of objects and they need to be retrained to categorize specific issues such as Covid-19 detection. In such models similar, ResNet, and SqueezeNet although the learning process is fast, it requires preprocessing the input image, size of the data set and setting multiple parameters. Color and edge features are extracted from the upper layers, and complex features are obtained from deeper layers. Due to the multiplicity of layers in transfer learning models, time consumption increases. The feature map and activation layers of the trained transfer learning model must be localized for the specific Covid-19 problem that requires a lot of memory [35]. After fine-tuning the pre-trained model principal component analysis (PCA), heuristic methods, automated encoders, and variance-based selectors could be used to select the optimal feature. Finally, ensemble methods such as a combination of SVMs or other classifiers can be used to predict the accuracy of Covid-19 disease diagnosis [36]. Using semi-supervised learning methods as self-learning may result in acceptable accuracy and less time spent labeling images [37].

For future work, using another feature selection algorithm and applying other learners may yield better results. In addition to the images, the parameters derived from the clinical trials can create a new model with a new combination of features to diagnose the disease or possibly predict its death. In addition to the images, the parameters extracted from the clinical trials can create a new model with a new combination of features, which may be effective in diagnosing the disease or possibly predicting its death.

Table 1. Average of a confusion matrix for 100 runs with 3 classes by the (a) optimized features (b) original features based on train, test, validation, and total data

(a) Optimized features

Optimized features test		Predicted		
		Covid	Normal	Pneumonia
actual	Covid	51/75	0	0/2
	Normal	0/15	54/9	0/1
	Pneumonia	0/4	0/55	55/95

Optimized features validation		Predicted		
		Covid	Normal	Pneumonia
actual	Covid	55/05	0/05	0/45
	Normal	0/05	54/4	0/3
	Pneumonia	0/4	1	52/3

Optimized features train		Predicted		
		Covid	Normal	Pneumonia
actual	Covid	256/5	0	0
	Normal	0	254/1	0
	Pneumonia	0	0	253/4

Optimized features total		Predicted		
		Covid	Normal	Pneumonia
Actual	Covid	363/3	0/05	0/65
	Normal	0/2	363/4	0/4
	Pneumonia	0/8	1/55	361/65

(b) Original features

Original features test		Predicted		
		Covid	Normal	Pneumonia
Actual	Covid	51/65	0	0/3
	Normal	0/25	54/65	0/25
	Pneumonia	0/5	0/95	55/45

original features validation		Predicted		
		Covid	Normal	Pneumonia
actual	Covid	54/85	0	0/7
	Normal	0/15	54/2	0/4
	Pneumonia	0/55	1/2	51/95

Original features train		Predicted		
		Covid	Normal	Pneumonia
Actual	Covid	256/45	0	0/05
	Normal	0	254/1	0
	Pneumonia	0	0	253/4

original features total		Predicted		
		Covid	Normal	Pneumonia
actual	Covid	362/95	0	1/05
	Normal	0/4	362/95	0/65
	Pneumonia	1/05	2/15	360/8

Table 2. Comparison of indicators (TP, TN, FP, FN, accuracy, the area under curve, sensitivity, specificity, geometric mean) for any output class based on (a) optimized features (b) original features

(a) Optimized features

Optimized features –total	Covid	Normal	Pneumonia
TP	363/30	363/40	361/65
TN	727/00	726/40	726/95
FP	1/00	1/60	1/05
FN	0/70	0/60	2/35
Accuracy	99/84	99/80	99/69
Sensitivity	99/81	99/84	99/35
Specificity	99/86	99/78	99/86
geometric mean	99/84	99/81	99/60
area under curve	0/9984	0/9981	0/9961

Optimized features –train	Covid	Normal	pneumonia
TP	256/50	254/10	253/40
TN	507/50	509/90	510/60
FP	0/00	0/00	0/00
FN	0/00	0/00	0/00
Accuracy	100/00	100/00	100/00
Sensitivity	100/00	100/00	100/00
Specificity	100/00	100/00	100/00
geometric mean	100/00	100/00	100/00
area under curve	1/0000	1/0000	1/0000

Optimized features –test	Covid	Normal	Pneumonia
TP	51/75	54/90	55/95
TN	111/50	108/30	106/80
FP	0/55	0/55	0/30
FN	0/20	0/25	0/95
Accuracy	99/54	99/51	99/24
Sensitivity	99/62	99/55	98/33
Specificity	99/51	99/49	99/72
geometric mean	99/56	99/52	99/02
area under curve	0/9956	0/9952	0/9903

Optimized features -valid	Covid	Normal	Pneumonia
TP	55/05	54/40	52/30
TN	108/00	108/20	109/55
FP	0/45	1/05	0/75
FN	0/50	0/35	1/40
Accuracy	99/42	99/15	98/69
Sensitivity	99/10	99/36	97/39
Specificity	99/59	99/04	99/32
geometric mean	99/34	99/20	98/35
area under curve	0/9934	0/9920	0/9840

(b) Original features

Original features -total	Covid	Normal	Pneumonia
TP	362/95	362/95	360/80
TN	726/55	725/85	726/30
FP	1/45	2/15	1/70
FN	1/05	1/05	3/20
Accuracy	99/77	99/71	99/55
Sensitivity	99/71	99/71	99/12
Specificity	99/80	99/70	99/77
geometric mean	99/76	99/71	99/44
area under curve	0/9976	0/9971	0/9944

Original features -train	Covid	Normal	pneumonia
TP	256/45	254/10	253/40
TN	507/50	509/90	510/55
FP	0/00	0/00	0/05
FN	0/05	0/00	0/00
Accuracy	99/99	100/00	99/99
Sensitivity	99/98	100/00	100/00
Specificity	100/00	100/00	99/99
geometric mean	99/99	100/00	100/00
area under curve	0/9999	1/0000	1/0000

Original features -test	Covid	Normal	Pneumonia
TP	51/65	54/65	55/45
TN	111/30	107/90	106/55
FP	0/75	0/95	0/55
FN	0/30	0/50	1/45
Accuracy	99/36	99/12	98/78
Sensitivity	99/42	99/09	97/45
Specificity	99/33	99/13	99/49
geometric mean	99/38	99/11	98/46
area under curve	0/9937	0/9910	0/9847

Original features -valid	Covid	Normal	Pneumonia
TP	54/85	54/20	51/95
TN	107/75	108/05	109/20
FP	0/70	1/20	1/10
FN	0/70	0/55	1/75
Accuracy	99/15	98/93	98/26
Sensitivity	98/74	99/00	96/74
Specificity	99/35	98/90	99/00
geometric mean	99/05	98/95	97/87
area under curve	0/9904	0/9895	0/9789

Table 3. Average of confusion matrix components for 100 runs by the original features and optimized features

Method	TP	TN	FP	FN	Accuracy	Sensitivity	Specificity	Geometric mean	Area Under Curve	RMSE
Original features by Deep convolution										
Training	254/65	509/32	0/02	0/02	1/0000	0/9999	1/0000	1/0000	0/9999	0/0036
Testing	53/92	108/58	0/75	0/75	0/9909	0/9866	0/9931	0/9898	0/9898	0/1533
Validation	53/67	108/33	1/00	1/00	0/9878	0/9816	0/9909	0/9862	0/9863	0/1905
Total	362/23	726/23	1/77	1/77	0/9968	0/9951	0/9976	0/9964	0/9964	1/1543
Optimized features by Binary Deferential										
Training	254/67	509/33	0/00	0/00	1/0000	1/0000	1/0000	1/0000	1/0000	0/0000
Testing	54/20	108/87	0/47	0/47	0/9943	0/9916	0/9957	0/9937	0/9937	0/1133
Validation	53/92	108/58	0/75	0/75	0/9909	0/9862	0/9931	0/9896	0/9898	0/1592
Total	362/78	726/78	1/22	1/22	0/9978	0/9967	0/9983	0/9975	0/9975	1/1543

Table 4. Comparison of the suggested approach with prior related research

research	Method	Number of features	Accuracy	Geometric mean	RAM	Max Computation time
[17]	Binary particle swarm optimization -VGG19	448	99.38	-	16 gigabyte	2500s
Proposed method	Binary differential -cnn	308	99.43	99.37	4 gigabyte	2300s

6. CONCLUSION

The number of people with COVID-19 disease has rapidly expanded. Machine vision techniques and artificial intelligence play an essential role in diagnosing the disease and helping to treat it. The purpose of this paper was to develop a method for problem “COVID-19”. A data set of lung images, including three categories of pneumonia, COVID-19, healthy, were considered.

A deep convolution neural network consisting of 11 layers was applied to extract the features. Relevant features were selected by the binary differential meta-heuristic method, and unrelated features were removed. Lung X-ray images were classified based on these optimal features using a SVM classifier. This study showed that the accuracy indicator, and the number of relevant extracted features, had better performance on the same data than previous methods. The proposed model based on a deep neural network and meta-heuristic algorithm for feature selection can be used in other medical applications.

Acknowledgments

The authors are grateful to all study participants.

Authors' contributions

Iraji and Feizi-Derakhshi suggested the algorithm for image analysis; iraji implemented it and also analyzed the experimental results; Tanha provided clinical guidance; Iraji, Feizi-Derakhshi, and Tanha consulted the obtained result. All authors read and approved the final manuscript.

Funding

This research received no specific grant from any funding agency in the public, commercial, or not-for-profit sectors.

Availability of data and materials

The datasets used and analyzed during the current study are available from the corresponding author on reasonable request.

DISCLOSURE OF POTENTIAL CONFLICTS OF INTEREST

Conflicts of interest

The authors declared no potential conflicts of interest with respect to the research, authorship, and/or publication of this article.

Ethical approval

This article does not contain any data, or other information from studies or experimentation, with the involvement of human or animal subjects.

Consent for publication

Agreed by the authors.

Competing interests

The authors declare that they have no competing interests.

REFERENCES

- 1 Sahlol, A.T., Yousri, D., Ewees, A.A., Al-Qaness, M.A., Damasevicius, R., and Abd Elaziz, M.: 'COVID-19 image classification using deep features and fractional-order marine predators algorithm', *Scientific Reports*, 2020, 10, (1), pp. 1-15
- 2 Hoque, N., Bhattacharyya, D.K., and Kalita, J.K.: 'MIFS-ND: A mutual information-based feature selection method', *Expert Systems with Applications*, 2014, 41, (14), pp. 6371-6385
- 3 Dey, N.: 'Advancements in applied metaheuristic computing' (IGI Global, 2017. 2017)
- 4 Lambin, P., Rios-Velazquez, E., Leijenaar, R., Carvalho, S., Van Stiphout, R.G., Granton, P., Zegers, C.M., Gillies, R., Boellard, R., and Dekker, A.: 'Radiomics: extracting more information from medical images using advanced feature analysis', *European journal of cancer*, 2012, 48, (4), pp. 441-446
- 5 Chong, D.Y., Kim, H.J., Lo, P., Young, S., McNitt-Gray, M.F., Abtin, F., Goldin, J.G., and Brown, M.S.: 'Robustness-driven feature selection in classification of fibrotic interstitial lung disease patterns in computed tomography using 3D texture features', *IEEE transactions on medical imaging*, 2015, 35, (1), pp. 144-157
- 6 Acharya, U.R., Fernandes, S.L., WeiKoh, J.E., Ciaccio, E.J., Fabbell, M.K.M., Tanik, U.J., Rajinikanth, V., and Yeong, C.H.: 'Automated detection of Alzheimer's disease using brain MRI images—a study with various feature extraction techniques', *Journal of Medical Systems*, 2019, 43, (9), pp. 302
- 7 Afzali, A., Mofrad, F.B., and Pouladian, M.: 'Feature Selection for Contour-based Tuberculosis Detection from Chest X-Ray Images', in Editor (Ed.)[^](Eds.): 'Book Feature Selection for Contour-based Tuberculosis Detection from Chest X-Ray Images' (IEEE, 2019, edn.), pp. 194-198
- 8 Da Silva, S.F., Ribeiro, M.X., Neto, J.d.E.B., Traina-Jr, C., and Traina, A.J.: 'Improving the ranking quality of medical image retrieval using a genetic feature selection method', *Decision support systems*, 2011, 51, (4), pp. 810-820
- 9 Li, J., Fong, S., Liu, L.-s., Dey, N., Ashour, A.S., and Moraru, L.: 'Dual feature selection and rebalancing strategy using metaheuristic optimization algorithms in X-ray image datasets', *Multimedia Tools and Applications*, 2019, 78, (15), pp. 20913-20933
- 10 Johnson, D.S., Johnson, D.L.L., Elavarasan, P., and Karunanithi, A.: 'Feature Selection Using Flower Pollination Optimization to Diagnose Lung Cancer from CT Images', in Editor (Ed.)[^](Eds.): 'Book Feature Selection Using Flower Pollination Optimization to Diagnose Lung Cancer from CT Images' (Springer, 2020, edn.), pp. 604-620
- 11 Hemdan, E.E.-D., Shouman, M.A., and Karar, M.E.: 'Covidx-net: A framework of deep learning classifiers to diagnose covid-19 in x-ray images', *arXiv preprint arXiv:2003.11055*, 2020
- 12 Toğaçar, M., Ergen, B., and Cömert, Z.: 'COVID-19 detection using deep learning models to exploit Social Mimic Optimization and structured chest X-ray images using fuzzy color and stacking approaches', *Computers in Biology and Medicine*, 2020, pp. 103805
- 13 Zhang, J., Xie, Y., Li, Y., Shen, C., and Xia, Y.: 'Covid-19 screening on chest x-ray images using deep learning based anomaly detection', *arXiv preprint arXiv:2003.12338*, 2020
- 14 Apostolopoulos, I.D., and Mpesiana, T.A.: 'Covid-19: automatic detection from x-ray images utilizing transfer learning with convolutional neural networks', *Physical and Engineering Sciences in Medicine*, 2020, pp. 1
- 15 Ozturk, T., Talo, M., Yildirim, E.A., Baloglu, U.B., Yildirim, O., and Acharya, U.R.: 'Automated detection of COVID-19 cases using deep neural networks with X-ray images', *Computers in Biology and Medicine*, 2020, pp. 103792
- 16 Heidari, M., Mirniaharikandehi, S., Khuzani, A.Z., Danala, G., Qiu, Y., and Zheng, B.: 'Improving the performance of CNN to predict the likelihood of COVID-19 using chest X-ray images with preprocessing algorithms', *International journal of medical informatics*, 2020, 144, pp. 104284

- 17 Canayaz, M.: 'MH-COVIDNet: Diagnosis of COVID-19 using deep neural networks and meta-heuristic-based feature selection on X-ray images', *Biomedical Signal Processing and Control*, 2020, 64, pp. 102257
- 18 Gao, Y., Zhu, T., and Xu, X.: 'Bone age assessment based on deep convolution neural network incorporated with segmentation', *International Journal of Computer Assisted Radiology and Surgery*, 2020, 15, (12), pp. 1951-1962
- 19 Adem, K., Kiliçarslan, S., and Cömert, O.: 'Classification and diagnosis of cervical cancer with stacked autoencoder and softmax classification', *Expert Systems with Applications*, 2019, 115, pp. 557-564
- 20 Khaire, U.M., and Dhanalakshmi, R.: 'High-dimensional microarray dataset classification using an improved adam optimizer (iAdam)', *Journal of Ambient Intelligence and Humanized Computing*, 2020, 11, (11), pp. 5187-5204
- 21 Ali, M.N.Y., Sarowar, M.G., Rahman, M.L., Chaki, J., Dey, N., and Tavares, J.M.R.: 'Adam deep learning with SOM for human sentiment classification', *International Journal of Ambient Computing and Intelligence (IJACI)*, 2019, 10, (3), pp. 92-116
- 22 Storn, R., and Price, K.: 'Differential evolution—a simple and efficient heuristic for global optimization over continuous spaces', *Journal of global optimization*, 1997, 11, (4), pp. 341-359
- 23 Zorarpaci, E., and Özel, S.A.: 'A hybrid approach of differential evolution and artificial bee colony for feature selection', *Expert Systems with Applications*, 2016, 62, pp. 91-103
- 24 Cohen, J.P., Morrison, P., Dao, L., Roth, K., Duong, T.Q., and Ghassemi, M.: 'Covid-19 image data collection: Prospective predictions are the future', *arXiv preprint arXiv:2006.11988*, 2020
- 25 Chowdhury, M.E., Rahman, T., Khandakar, A., Mazhar, R., Kadir, M.A., Mahbub, Z.B., Islam, K.R., Khan, M.S., Iqbal, A., and Al-Emadi, N.: 'Can AI help in screening viral and COVID-19 pneumonia?', *arXiv preprint arXiv:2003.13145*, 2020
- 26 Kermany, D., Zhang, K., and Goldbaum, M.: 'Labeled optical coherence tomography (OCT) and Chest X-Ray images for classification', *Mendeley data*, 2018, 2
- 27 Rajinikanth, V., Dey, N., Raj, A.N.J., Hassanien, A.E., Santosh, K., and Raja, N.: 'Harmony-search and otsu based system for coronavirus disease (COVID-19) detection using lung CT scan images', *arXiv preprint arXiv:2004.03431*, 2020
- 28 Dey, N., Rajinikanth, V., Fong, S.J., Kaiser, M.S., and Mahmud, M.: 'Social group optimization—assisted Kapur's entropy and morphological segmentation for automated detection of COVID-19 infection from computed tomography images', *Cognitive Computation*, 2020, 12, (5), pp. 1011-1023
- 29 Farag, A.A., Ali, A., Elshazly, S., and Farag, A.A.: 'Feature fusion for lung nodule classification', *International journal of computer assisted radiology and surgery*, 2017, 12, (10), pp. 1809-1818
- 30 Li, Z., Jiang, J., Zhou, H., Zheng, Q., Liu, X., Chen, K., Weng, H., and Chen, W.: 'Development of a deep learning-based image eligibility verification system for detecting and filtering out ineligible fundus images: A multicentre study', *International Journal of Medical Informatics*, 2021, 147, pp. 104363
- 31 Xu, L., Wang, X., Bai, L., Xiao, J., Liu, Q., Chen, E., Jiang, X., and Luo, B.: 'Probabilistic SVM classifier ensemble selection based on GMDH-type neural network', *Pattern Recognition*, 2020, 106, pp. 107373
- 32 Er, O., Tanrikulu, A.C., Abakay, A., and Temurtas, F.: 'An approach based on probabilistic neural network for diagnosis of Mesothelioma's disease', *Computers & Electrical Engineering*, 2012, 38, (1), pp. 75-81
- 33 Temurtas, H., Yumusak, N., and Temurtas, F.: 'A comparative study on diabetes disease diagnosis using neural networks', *Expert Systems with applications*, 2009, 36, (4), pp. 8610-8615
- 34 Kuncheva, L.I.: 'Combining pattern classifiers: methods and algorithms' (John Wiley & Sons, 2014. 2014)
- 35 Ahuja, S., Panigrahi, B.K., Dey, N., Rajinikanth, V., and Gandhi, T.K.: 'Deep transfer learning-based automated detection of COVID-19 from lung CT scan slices', *Applied Intelligence*, 2021, 51, (1), pp. 571-585

- 36 Singh, M., Bansal, S., Ahuja, S., Dubey, R.K., Panigrahi, B.K., and Dey, N.: 'Transfer learning–based ensemble support vector machine model for automated COVID-19 detection using lung computerized tomography scan data', *Medical & biological engineering & computing*, 2021, 59, (4), pp. 825-839
- 37 Konar, D., Panigrahi, B.K., Bhattacharyya, S., Dey, N., and Jiang, R.: 'Auto-diagnosis of covid-19 using lung ct images with semi-supervised shallow learning network', *IEEE Access*, 2021, 9, pp. 28716-28728